Received: 29 October 2021 | Revised: 25 January 2022 | Accepted: 3 February 2022

DOI: 10.1002/htj.22483

ORIGINAL ARTICLE

HEAT TRANSFER WILEY

Experimental investigation of transient thermal characteristics of a dry friction clutch using alternative friction materials under different operating conditions

Jenan S. Sherzaa[1] | **Ihsan Y. Hussain**[2] | **Oday I. Abdullah**[3,4,5]

[1]Air Conditioning Techniques Engineering Department, Al-Esraa University College, Baghdad, Iraq

[2]Mechanical Engineering Department, College of Engineering, University of Baghdad, Baghdad, Iraq

[3]Energy Engineering Department, College of Engineering, University of Baghdad, Baghdad, Iraq

[4]Department of Mechanics, Al-Farabi Kazakh National University, Almaty, Kazakhstan

[5]System Technologies and Engineering Design Methodology, Hamburg University of Technology, Hamburg, Germany

Correspondence
Oday I. Abdullah, System Technologies and Engineering Design Methodology, Hamburg University of Technology, Denickestraße 17 (L), Hamburg 21073, Germany.
Email: oday.abdullah@tuhh.de

Abstract

The thermal characteristics of four types of dry friction clutch materials (LUK, G95, HCC, and Tiger) are investigated experimentally and numerically in the present work under different working conditions; such as initial sliding angular velocity (ω_{ro}), torque (T), and sliding time (t_s). The temperature distributions over a cross-section of friction clutch elements (pressure plate and flywheel) are investigated and optimized during the sliding period (heating phase), and full engagement period (cooling phase). The effect of alternative frictional materials lining of a clutch disc on the thermal behavior of the sliding system under different operating conditions (different angular velocities, torques, and sliding periods) is investigated experimentally. The results showed that the maximum effect on the temperature values occurred when applying maximum torque (4.5 kg·m), maximum initial rotational speed (1200 rpm), slipping period (30 s). However, the temperature values at interface contact decrease when decreasing all the above input conditions values to (2.5 kg·m, 690 rpm, and slipping period to 8 s). The results showed that the temperature reduced (53%)

from (180.4°C) for applied torque 4.5 kg·m with initial rotational speed (1200 rpm) and slip period (30 s) to (83.3°C) when applied torque 2.5 kg·m, initial rotational speed (680 rpm) and slip period (8 s) for clutch disc (LUK). It was obtained the same behavior for the other three discs (G95, HCC, and Tiger), but with different values of temperatures. The results show that the temperatures of the pressure plate interface ($T_{max} = 159.1$°C) are higher than those at the flywheel interface ($T_{max} = 152.7$°C), due to the low thermal capacity of pressure plate compared to the flywheel when using G95 frictional material. The experimental optimization results showed that the highest temperatures were obtained when using friction clutch disc (LUK), and minimum temperature when using (HCC) disc, around (20%) reduction when replaced (LUK) material with (HCC) under the same working conditions ($T = 4.5$ kg·m, $\omega_{ro} = 1200$ rpm, and $t_s = 30$ s).

KEYWORDS
alternative fractional material, dry friction clutch, experimental work, FE analysis, temperature distribution

1 | INTRODUCTION

The field of automotive clutches and brakes is substantial in the automotive industry, which makes it a very important field for researchers to deal with. The temperatures of the rubbing surfaces increased rapidly due to the heat generated during sliding between two contacting surfaces. Temperatures that raise during the sliding period have a considerable influence on the lifetime of the sliding surfaces of the clutch. High thermal stresses will be produced at the contact surface due to increased values of surface temperatures. When the clutch continues working under these conditions, this situation causes surface cracks and permanent distortions. Therefore, it is necessary to know the magnitude of the maximum surface temperature to prevent or at least reduce the clutch failure before the lifetime, and how this depends on known conditions of loading.

By studying the effects of thermal expansion on the brakes, Barber[1] studied the hot spots that appear on the brake contact surfaces using two metal surfaces that collide with each other. His experiment showed that thermal distortion appears in the contact area between contact bodies caused by temperature fluctuations. Later, Barber[2] discovered a phenomenon known as thermoelastic instability (TEI) when he studied the effects of thermal expansion on the brakes. The experiments showed that when two bodies are nominally in contact over a large area and collide with one another, heat is generated because of friction. Surface roughness plays an

important role in changing contact pressure distribution and surface temperatures. Therefore, the contact pressure distribution will be affected, causing the distortion of the bodies by thermal expansion. The sliding system will be unstable if the heat generated by the friction is sufficiently high and the hot spots appear on the contact surfaces of the bodies in places where the contact pressure and temperature values are very high. Santini and Kennedy[3] studied the temperature field of contact surfaces considering the effect of wear. In their study, they used a rotor disc surrounded by two brake pads controlled by the calipers. Their experiments showed that there is a temperature gradient across the contact surface between the rotor and the pads, and the addition of a groove on the surface of the pads decreases the surface temperature and the rate of wear extensively. Their results have also shown that the contact surface between the pad and the disc is not uniform. At any time during the test, the effective contact area was less than 25% of the nominal contact area. Furthermore, they have shown that the use of a flexible spring-ring support behind the friction pads has improved wear rate, reduced surface temperature, and increased contact area. Anderson and Knopp[4] presented the types of hot spots on the brake surfaces. These types are asperity, focal, distorted, and regional. The studies included a finite element model for estimating temperature changes around hot spots at different intervals. They found that focal hot spots have a significant negative effect on brake performance. Furthermore, they have shown that the high sliding speed, the long contact time for friction, the low wear resistance of materials and thick materials lead to thermoelastic instability. Panier et al.[5] investigated the occurrence of hot spots on railway disc brakes using thermographic measurements with an infrared camera on the rubbing surface of the brake discs on a large-scale test bench. They also studied the effect of parameters such as the pad's stiffness and the pad's contact length in hot spots.

Abdullah and Schlattmann[6] studied experimentally and numerically the field of temperature and heat generation due to friction. In their work, they used a pin-on-disk test platform also three-dimensional finite element model was used to find heat generation and temperature distribution during the sliding operation. Their results showed the friction disc average temperature lower than the average temperature values of the steel pin and that happened because of the fact of using low thermal conductivity values of friction materials. In addition, the studies present a promising design tool to study the effect of the type of materials, surface roughness, boundary conditions, and temperatures depending on the properties of the material in the thermoelastic phenomena of sliding systems. Mouffak and Bouchetara[7] studied the temperature distribution for three models of clutches through the sliding time as well as for a single engagement, varying the friction material, the values of the pressure and the initial angular velocity to investigate the influences of these parameters on the sliding system. They also analyzed and modified the model of the clutch disc for minimizing the friction energy that converted to heat due to conduction and convection; to find solutions for a better clutch model.

Ali et al.[8] found the solution for the transient thermal problem of the dry clutch system using different materials. Their results presented the temperature distribution of friction during the beginning of the engagement. They obtained a numerical solution based on the finite element approach. They used ANSYS 15 software to compute the temperature distribution at any time of the slipping time. Gkinis et al.[9] enhanced an analytical solution of the thermal problem for dry friction clutch. They assumed that all kinetic energy during the slipping converted into heat led to increasing the surface temperature very quickly. They used the pin-on-disc test rig to find the magnitude of the friction coefficients under different working conditions. Two different assumptions were assumed: new frictional facing and used one.

They found that depletion of heat-conducting elements effect significantly on the stability of the system (judder, characteristics of frictional material).

Abdullah et al.[10] investigated the effect of frictional facing thickness of the clutch disc that consists of multiple friction discs on the contact pressure for all contacting surfaces at the beginning of engagement using a FE approach. They found that the frictional facing thickness has a great influence the elastic and thermal behavior of the muti-disc clutch system. They presented evidence about increasing the contact pressure significantly with decreasing the frictional facing thickness.

Sherza et al.[11] enhanced analytical solution to find the variation of frictional heat generated in the dry clutch system during the sliding time. They assumed that the pressure is uniform over the contact surfaces of the clutch and the sliding angular velocity is decreased with time of sliding linearly. They found that the frictional heat generated changed with disc radius, where the minimum value at inner radius and the maximum one at the out radius. Later on, Sherza et al.[12] studied the frictional heat generated and temperature history for the clutch disc, flywheel, and pressure plate; during the slipping period using ANSYS/Workbench software 18 depending on the fundamental design theories for friction clutch (uniform wear and uniform pressure). Assumed the torque during the sliding period was constant with time.

Al-Zubaidi and Abdullah[13] investigated the thermal effect on the frictional facing materials of the clutch disc experimentally. All their tests were conducted under dry working conditions. They found that high thermal levels decreased the frictional characteristics (coefficient of friction) of the material led to reducing the performance of the clutch system.

Biczó et al.[14] used a new frictional facing that consists of different materials such as fiberglass with copper and aromatic polyamide material to investigate the thermal and structural behavior of dry clutches. These components of materials were reinforced with acrylic nitrile. They studied the influence of temperature on the characteristics of friction materials. They found that each material has a different response with high temperatures. A number of researchers investigated various parameters of the friction materials and their effects on the thermal performance of dry friction clutches, for example, AL-Alawi et al.[15] studied the characteristics of material composed of a Cu-based, Ramesh et al.[16] suggested to use different frictional facing materials (e.g., G95, VH-03, SF-CPX61 & SF-MC2). Bhaduri and MuruguNachippan[17] presented detailed comparisons of thermal behaviors among different frictional facing (Sintered Iron, Molded Asbestos, F3S20S-T61, Al-MMC, Al-MMC & F3D20S-T5). While, Biczó et al.,[14] Bhandari and Mane[18] investigated the influence of using the fiber-reinforced hybrid composites (and focus on aluminum alloy, e.g., A-360), Harish and Kumar[19] studied the thermal behavior of clutches system using three different frictional materials (Asbestos, Kevlar 29, Sintered iron).

The present work consists of two main parts: build the new test rig of the dry friction clutch that has the ability to study the thermal performance of the clutch system for different configurations. The new test rig was validated with the numerical result obtained from the axisymmetric finite element model developed for this purpose. While, in the second part, it investigates experimentally the magnitude and distribution of the temperature for dry friction clutches during the sliding period when the transmitted torque by the clutch is variable. Different friction clutch materials are used (LUK, G95, HCC, and Tiger), each is characterized by different thermal and mechanical properties. The objective was to compare these materials and choose the optimal one in the design of a dry friction clutch. The parameters which affect the performance of clutches such as the sliding speed, slipping period, and torque capacity are investigated as well.

2 | EXPERIMENTAL APPARATUS AND PROCEDURE

It was designed and built a new test rig that was used in the present work. It consists of three main parts; the driving part, driven part, and the mechanical friction clutch which couples both parts as shown in Figure 1A,B. Also, there are measurements tools for clutch torque, pressure, and clutch friction interface temperatures. The driving part consists of Electrical-Motor

(A)

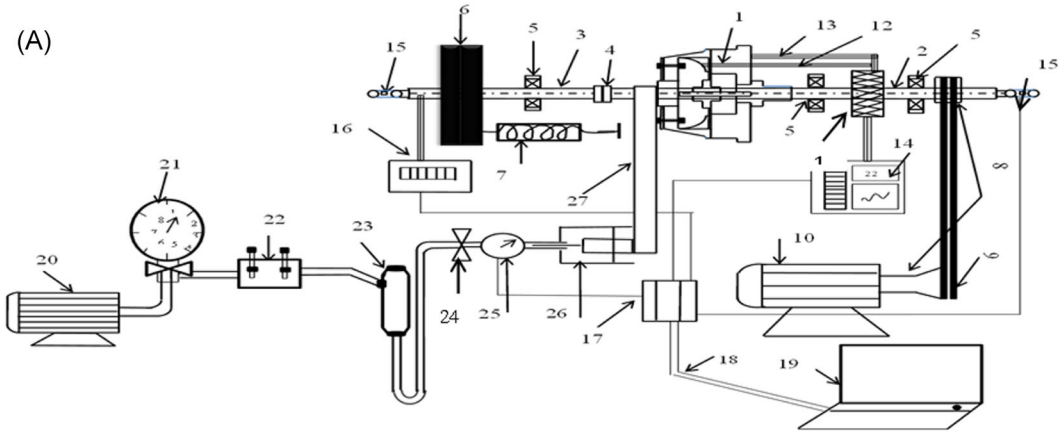

1	Clutch system	10	Electric motor	19	Computer
2	Input shaft	11	Slip ring	20	Air Compressor
3	Output shaft	12	Thermocouple from pressure plate	21	Air pressure regulator
4	Coupling	13	Thermocouple from flywheel	22	Solinoyed
5	Pillow block bearing unit	14	Data acquisition	23	Oil cylinder
6	Driven part	15	Velocity transducer	24	Throttle valve
7	System of applied torque	16	Torque measurement	25	Pressure transducer
8	Pulley	17	Arduino boards (controller)	26	Piston
9	Belt	18	USB	27	Link to pressure plate

(B)

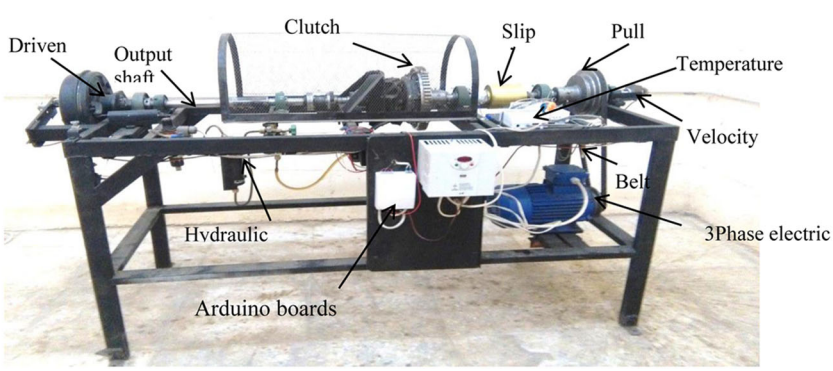

FIGURE 1 (A) Schematic for the experimental test rig and (B) photo of the experimental apparatus

(3 phases, 10 hp) with the speed of 1500 rpm that drives the clutch via a coupling that is torsion stiff. Its speed is controlled mechanically by using pulleys and belts. The driven part is working as a generator, which provides controlled application of the power. In this system, the Peugeot disc brake is used as a generator, which causes appropriate anti-torque depending on a connecting load. The apparatus was placed in Graduate Laboratory at the Mechanical Engineering Department—College of Engineering—the University of Baghdad, where all tests were made.

A single-disc dry friction clutch (axial friction clutches) is used. The main parts of a single disc clutch system are; pressure plate, clutch disc (four different friction clutch disc materials were used named [G95, LUK, HCC, and Tiger]), and flywheel. The frictional clutch disc is faced with a friction material from both sides. The clutch disc mounted on the hub is free to move in the axial direction along the splines of the driven shaft. The pressure plate is mounted inside the clutch system and is bolted to the flywheel. Both the pressure plate and the flywheel rotate together with the driving shaft. The normal force or surface pressure needed to transmit torque is controlled with a hydraulic cylinder. When the normal force is applied to the clutch by the hydraulic cylinder, torque is transmitted from the driving shaft to the output shaft. The transmitted torque is then measured by a means of a strain-gauge reactive torque sensor. The applied normal force is measured by a pressure transducer. The clutch slip speed is measured by using a high-resolution speed transducer placed at the differential input. K-type thermocouples are placed at six holes drilled in the rotating flywheel and the pressure plate to measure the interface temperatures of clutch friction. A slip ring was used to connect these thermocouples. The slip ring transmits the electrical signal from the rotating shaft to the fixed body. It consists of two parts; the rotor (connected with the rotating shaft) and the stator (connected with the fixed body). The slip ring is of 24-channels and is manufactured by MOFLON Technology Company Limited. The inner diameter is 40 mm. It works with 20,000 rpm maximum rotation speed and range of working temperature (−40 to −200)°C.

The actuation is a hydraulic type (the fluid pressure drives the piston to mechanical engagement or disengagement). The hydraulic system consists of an air compressor, regulator, solenoid, cylindrical oil tank, valve, and piston as shown in Figure 2. The Air compressor which provides the system with air is of Model: 2C- 0.1218, 2 hp and works in single-phase (220–240 V, 50–60 Hz) with maximum pressure 8 bar, tank capacity of 25 L, and displacement (120 L/min). Air pressure regulator is used to regulate the air pressure and thus control the speed of interconnection and isolation of the pressure plate. A cylindrical oil tank is used to convert the pressure of the air to oil pressure and thus

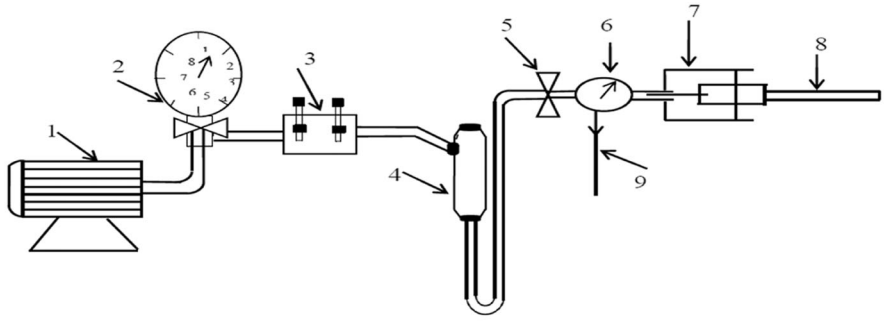

1	Air compressor	4	Oil cylinder	7	Piston
2	Air pressure regulator	5	Throttle valve	8	Link to pressure plate
3	Solinoyed	6	Pressure transducer	9	Signal to controller

FIGURE 2 Schematic of the hydraulic cylinder system

regulate the flow of oil. The throttle valve is the regulator of oil flow to control the slipping period. A piston is used to convert oil pressure energy to kinetic energy. Through this system, the engagement and disengagement processes can be controlled between the clutch parts. During the engagement, the pressure plate pushes the friction plate using a diaphragm spring onto the flywheel which is mounted on the driving shaft, hence providing torque and speed transmission. During the disengagement, pressure releases friction plate from flywheel thus disrupting the flow of power.

To obtain a clear conception of how the temperature is distributed, twelve thermocouples have been installed on the surface of the clutch, six thermocouples distributed on the flywheel side, and the other six on the pressure plate side, as shown in Figure 3. To install the thermocouples, holes were made in both the surface of the flywheel and the pressure plate, and through these holes; the thermocouples were fixed to the nearest contact points between the two surfaces (clutch disc-flywheel and pressure plate-clutch disc). The thermocouples distribution was as follows; three thermocouples in r-direction and the other three in θ-direction, see Figure 3. It was used thermocouples of type K, where they have the same probe diameter (0.5 mm). The thermocouples were connected to a data acquisition system, consisting of a 12-channel temperature recorder (Model MAX 6675 ISA) that performs cold-junction compensation and digitalizes the signal from a type-k thermocouple. The data output is with a 12-bit resolution. This converter resolves temperatures to 0.25°C, allows reading as high as +1024°C. A heat conductor (grease) was used on the head of the thermocouple to increase the thermal conductance and an insulator (silicon) on the remaining parts to ensure highly accurate results.

The experimental procedure was designed to investigate the effect of different types of frictional clutch disc materials on the behavior of the sliding system with different input conditions such as (velocity, torque, axial force, and sliding period). The values of investigated parameters are given in Table 1.

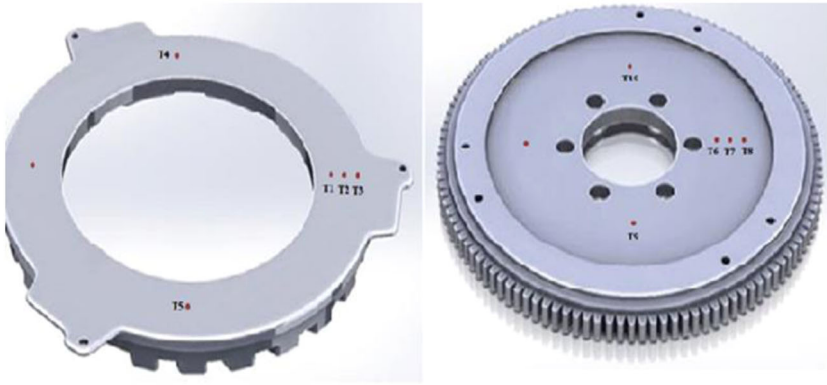

FIGURE 3 Thermocouple distribution on pressure plate and flywheel surface

TABLE 1 The performed experiments

Variable parameters frictional material	Velocity (rpm)	Torque (kg·m)	Slip time (s)
Disk 1 (G95)	1200, 860, 680	4.5, 3.5, 2.5	30, 20, 15, 8
Disk 2 (HCC)	1200, 860, 680	4.5, 3.5, 2.5	30, 20, 15, 8
Disk 3 (Tiger)	1200, 860, 680	4.5, 3.5, 2.5	30, 20, 15, 8
Disk 4 (LUK)	1200, 860, 680	4.5, 3.5, 2.5	30, 20, 15, 8

TABLE 2 Properties of the clutch disc materials

Materials	HCC	G95	LUK	Tiger
Friction coefficient	0.45	0.55	0.3	0.3
Modulus of elasticity (GPa)	310	305	490	420
Specific heat (J/kg·K)	900	935	1010	1780
Thermal conductivity (W/m·K)	33	24	0.4378	0.726
Density (kg/m^3)	1950	1870	1734	1570

3 | ALTERNATIVE FRICTION MATERIALS

To improve the clutch performance and increase the lifetime for frictional facings of clutch, a friction material with good mechanical and thermal properties must be chosen. A suitable friction material should provide a high coefficient of friction, should have an acceptable rate of wear, and withstand high temperatures. Thermal properties of friction material play an important role in the process of the designing of clutches. The good thermal conductivity and thermal diffusivity as well as high specific heat are important to increase the lifetime of friction material of clutch. To obtain environmentally friendly friction material with desired thermal and mechanical properties in the design, so it was selected the frictional materials that are available and have good properties. Two discs were imported with different thermal and mechanical properties. The first one is G95, that used typically for automotive clutch applications. Under normal operating conditions, G95 is a very reliable, hard-wearing, and economic material. The glass fiber reinforcement yarn is spiral woven with a fine copper core to produce a strong material with good heat transfer characteristics. G95 facings combine high resistance of bursting with smooth behavior. The second disc is HCC, which is a special woven material that is designed to work at high temperatures and has a low rate of wear. Where it was reinforced with extra copper to increase friction performance. HCC can dissipate heat, has a very stable friction coefficient, and steady work at high temperatures with minimal wear. The other discs are G59 and HCC). The properties of selected frictional facing materials are listed in Table 2.

4 | RESULTS AND DISCUSSIONS

Results obtained from experimentally designed systems are presented and analyzed for several parameters to study the influence of each of them on the thermal performance of friction clutch. Four different frictional facings (G95, LUK, HCC, and Tiger) were used to achieve the experimental work. In general, the temperature distribution and heat flux generated at the interface of the contact between the clutch parts are influenced by material properties, angular sliding velocity, slipping time, pressure capacity (torque) and disc radius.

Figures 4–51 illustrate the variation of surface temperature with time for the selected frictional material applying different values of torque (4.5, 3.5, and 2.5 kg·m) with fixed angular velocity and slip time. The first set of Figures 4–23 presents the thermal behavior of the clutch system when angular sliding velocity was 1200 rpm and slipping period was 30 s. While the second set of Figures 24–51, the angular velocity was 680 rpm and slipping period was 8 s.

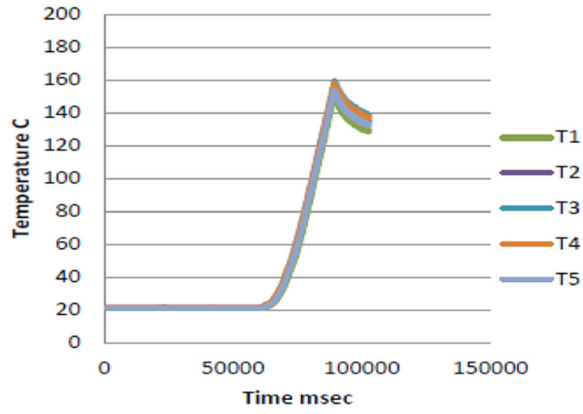

FIGURE 4 Temperature distribution on the pressure plate surface (slip time, 30 s; relative velocity, 1200 rpm; and torque, 4.5 kg·m) for G95 Disc

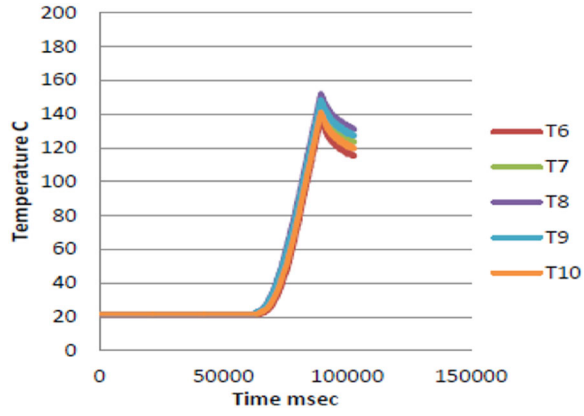

FIGURE 5 Temperature distribution on the flywheel surface (slip time, 30 s; relative velocity, 1200 rpm; and torque, 4.5 kg·m) for G95 Disc

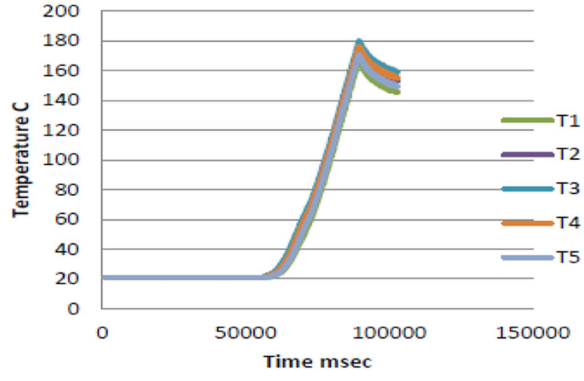

FIGURE 6 Temperature distribution on the pressure plate surface (slip time, 30 s; relative velocity, 1200 rpm; and torque, 4.5 kg·m) for LUK disc

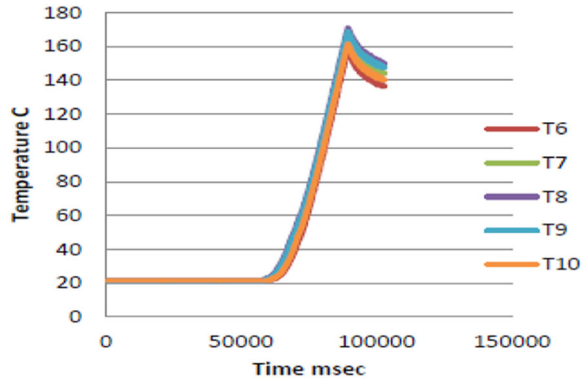

FIGURE 7 Temperature distribution on the flywheel surface (slip time, 30 s; relative velocity, 1200 rpm; and torque, 4.5 kg·m) for LUK disc

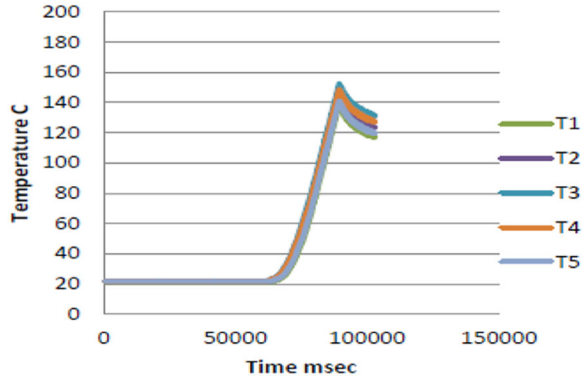

FIGURE 8 Temperature distribution on the pressure plate surface (slip time, 30 s; relative velocity, 1200 rpm; and torque, 4.5 kg·m) for HCC disc

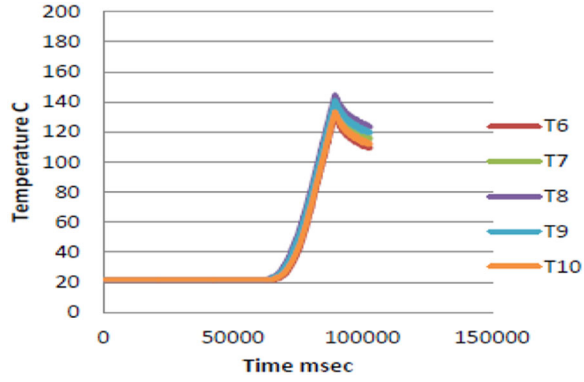

FIGURE 9 Temperature distribution on the flywheel surface (slip time, 30 s; relative velocity, 1200 rpm; and torque, 4.5 kg·m) for HCC disc

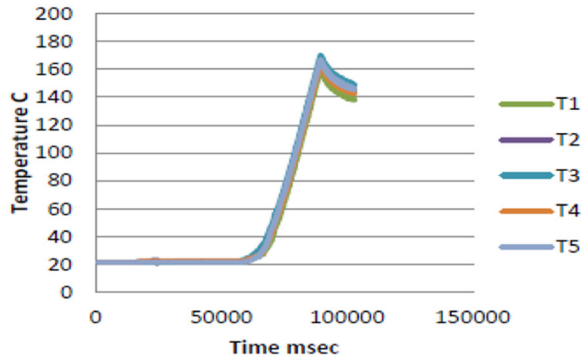

FIGURE 10 Temperature distribution on the pressure plate surface (slip time, 30 s; relative velocity, 1200 rpm; and torque, 4.5 kg·m) for Tiger disc

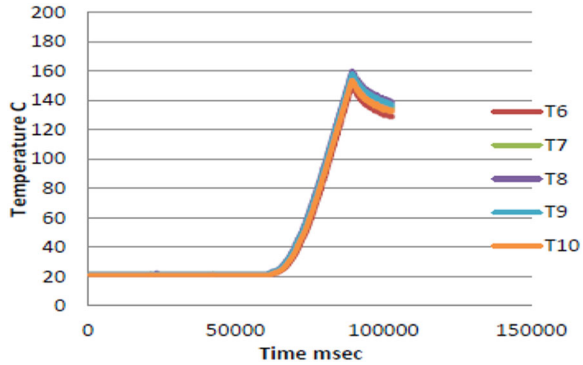

FIGURE 11 Temperature distribution on the flywheel surface (slip time, 30 s; relative velocity, 1200 rpm; and torque, 4.5 kg·m) for Tiger disc

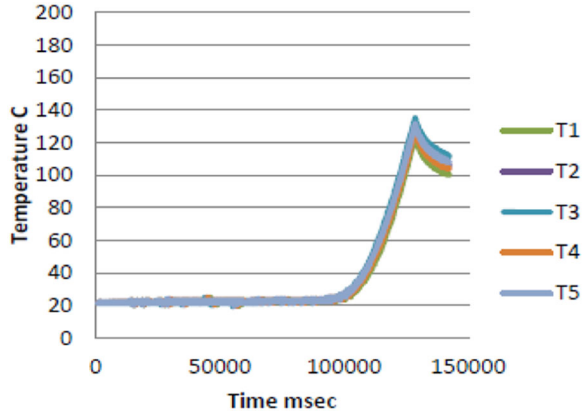

FIGURE 12 Temperature distribution on the pressure plate surface (slip time, 30 s; relative velocity, 1200 rpm; and torque, 3.5 kg·m) for G95 disc

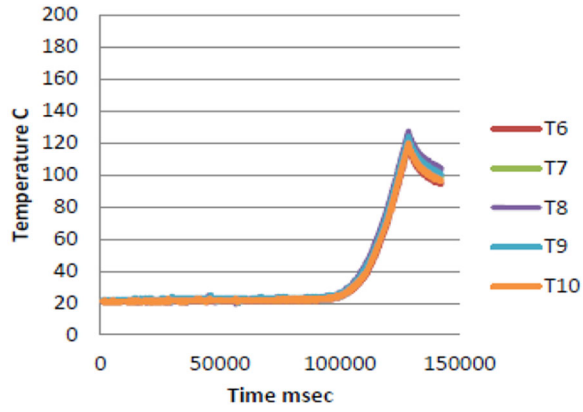

FIGURE 13 Temperature distribution on the flywheel surface (slip time, 30 s; relative velocity, 1200 rpm; and torque, 3.5 kg·m) for G95 disc

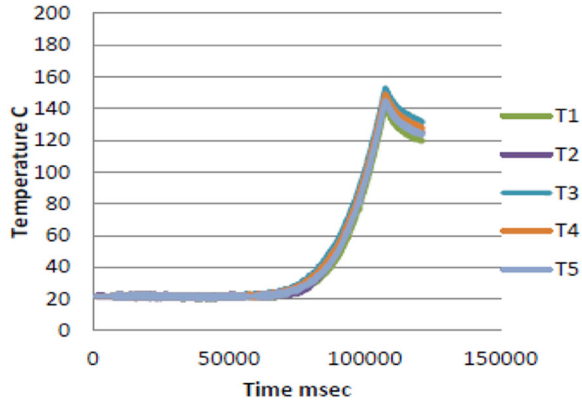

FIGURE 14 Temperature distribution on the pressure plate surface (slip time, 30 s; relative velocity, 1200 rpm; and torque, 3.5 kg·m) for LUK disc

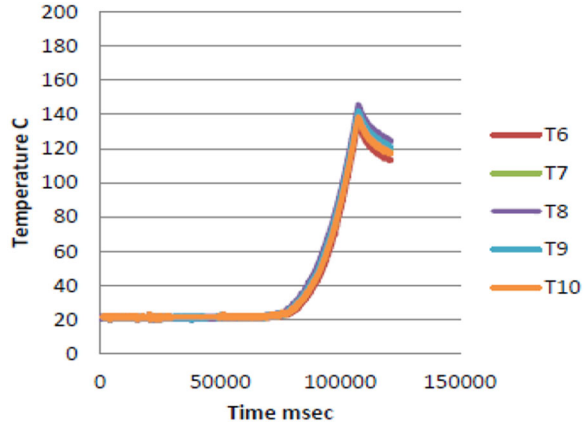

FIGURE 15 Temperature distribution on the flywheel surface (slip time, 30 s; relative velocity, 1200 rpm; and torque 3.5 kg·m) for LUK disc

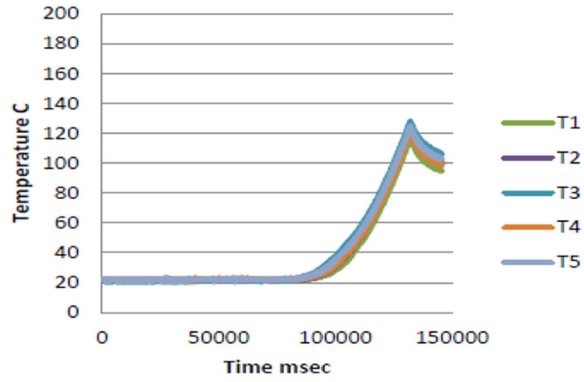

FIGURE 16 Temperature distribution on the pressure plate surface (slip time, 30 s; relative velocity, 1200 rpm; and torque. 3.5 kg·m) for HCC disc

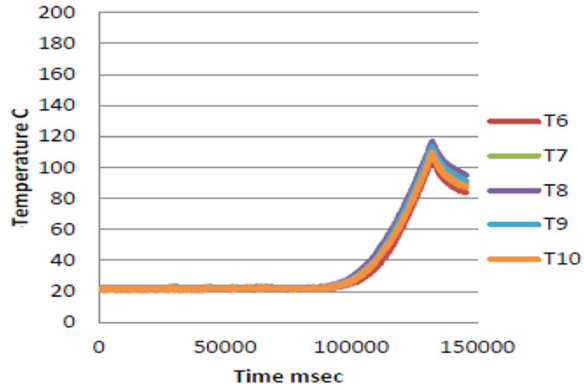

FIGURE 17 Temperature distribution on the flywheel surface (slip time, 30 s; relative velocity, 1200 rpm; and torque, 3.5 kg·m) for HCC disc

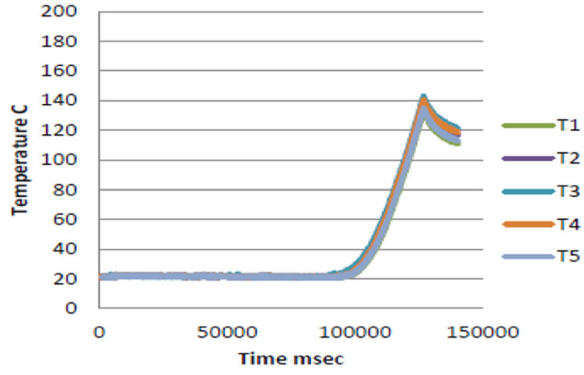

FIGURE 18 Temperature distribution on the pressure plate surface (slip time, 30 s; relative velocity, 1200 rpm; and torque, 3.5 kg·m) for Tiger disc

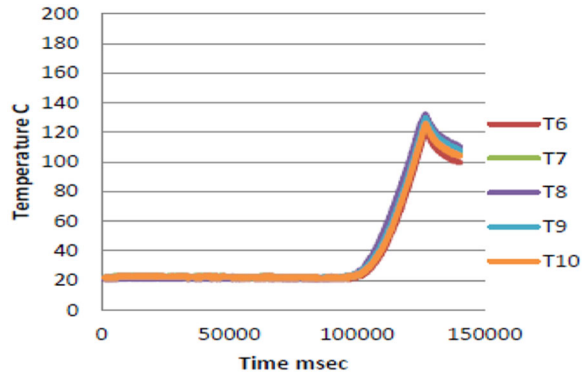

FIGURE 19 Temperature distribution on the flywheel surface (slip time, 30 s; relative velocity, 1200 rpm; and torque, 3.5 kg·m) for Tiger disc

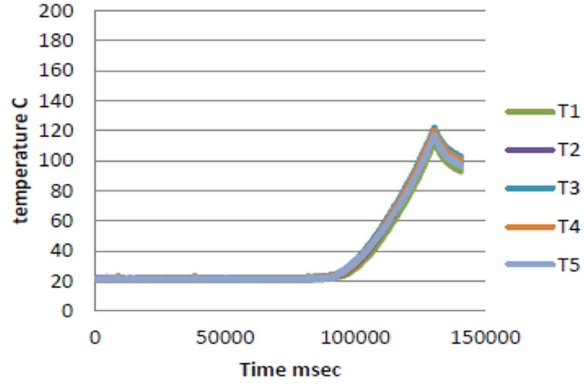

FIGURE 20 Temperature distribution on the pressure plate surface (slip time, 30 s; relative velocity, 1200 rpm; and torque, 2.5 kg·m) for G95 disc

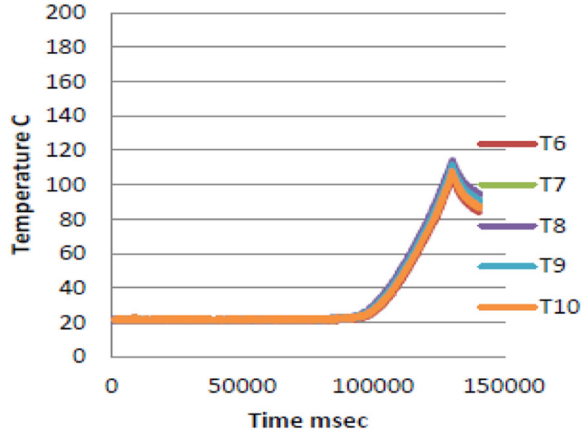

FIGURE 21 Temperature distribution on the flywheel surface (slip time, 30 s; relative velocity, 1200 rpm; and torque, 2.5 kg·m) for G95 disc

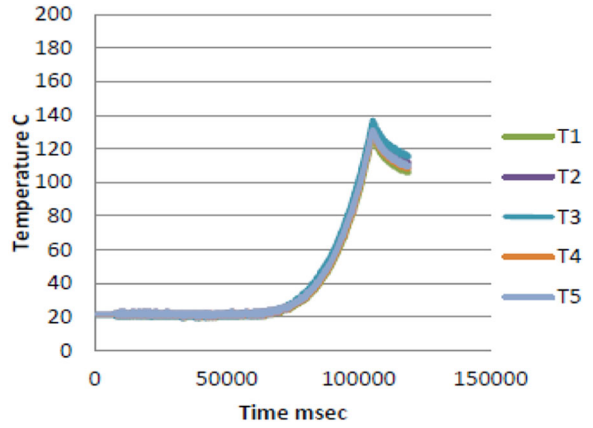

FIGURE 22 Temperature distribution on the pressure plate surface (slip time, 30 s; relative velocity, 1200 rpm; and torque, 2.5 kg·m) for LUK disc

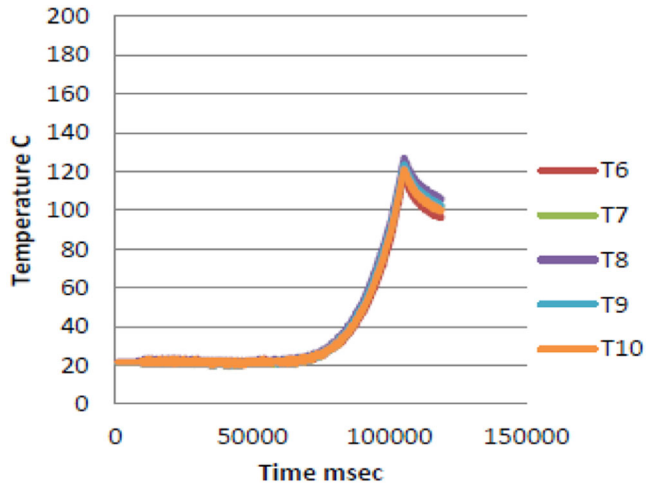

FIGURE 23 Temperature distribution on the flywheel surface (slip time, 30 s; relative velocity, 1200 rpm; and torque, 2.5 kg·m) for LUK disc

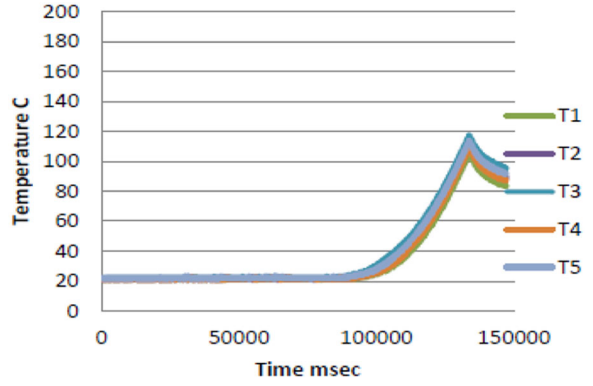

FIGURE 24 Temperature distribution on the pressure plate surface (slip time, 30 s; relative velocity, 1200 rpm; and torque, 2.5 kg·m) for HCC disc

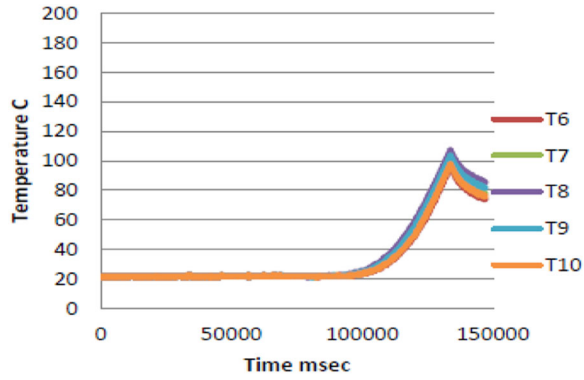

FIGURE 25 Temperature distribution on the flywheel surface (slip time, 30 s; relative velocity, 1200 rpm; and torque, 2.5 kg·m) for HCC disc

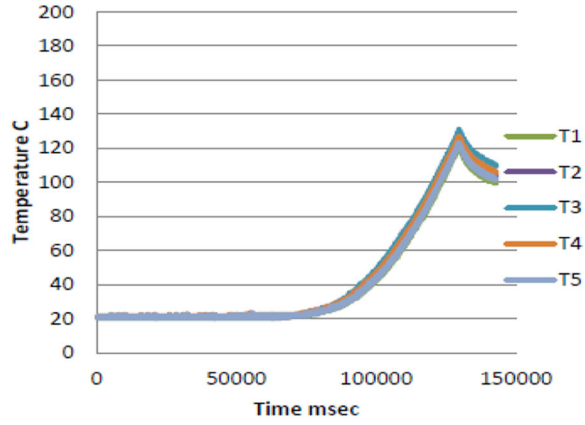

FIGURE 26 Temperature distribution on the pressure plate surface (slip time, 30 s; relative velocity, 1200 rpm; and torque, 2.5 kg·m) for Tiger disc

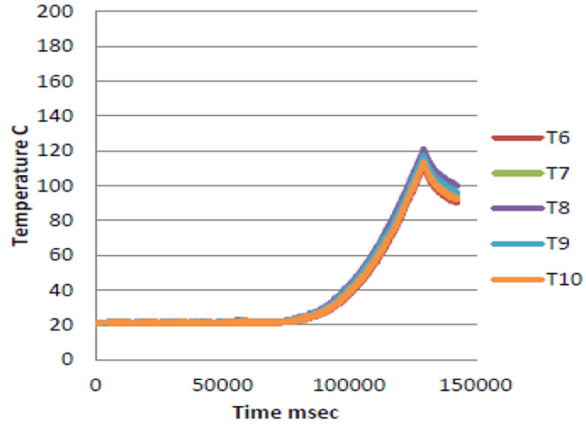

FIGURE 27 Temperature distribution on the flywheel surface (slip time, 30 s; relative velocity, 1200 rpm; and torque, 2.5 kg·m) for Tiger disc

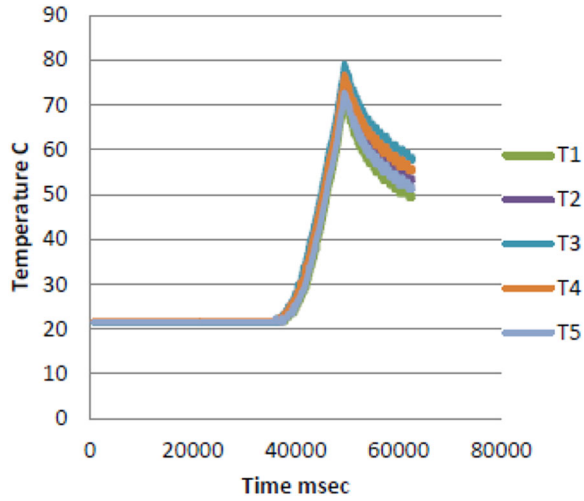

FIGURE 28 Temperature distribution on the pressure plate surface (slip time, 8 s; relative velocity, 680 rpm; and torque, 4.5 kg·m) for G95 disc

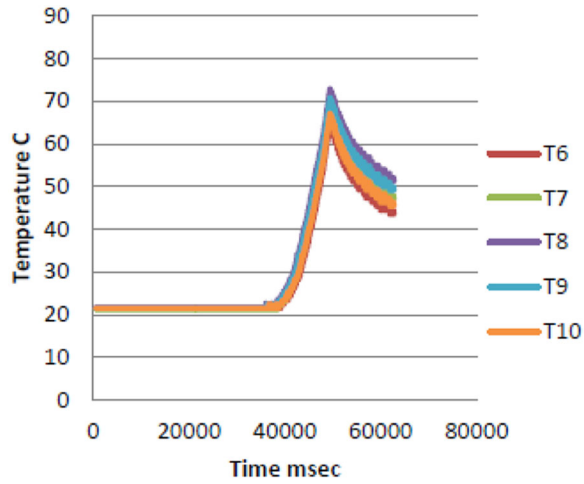

FIGURE 29 Temperature distribution on the flywheel surface (slip time, 8 s; relative velocity, 680 rpm; and torque, 4.5 kg·m) for G95 disc

These tests were focused to demonstrate the effect of high torque values on the performance and thermal behavior of friction clutch with constant angular speed and slip time.

It can be seen from the results that the maximum effect on the temperature values occurred when applying the highest torque (4.5 kg·m); where the temperature values grew very quickly with time when the values of applied torque increased. This happened because of the amount of frictional heat generation is directly dependent on the applied torque on the clutch disc.

It can be seen from Figures 4, 12, and 20 that the highest values of temperature are found (159.1°C, 135.4°C, and 122.5°C) that correspond to the applying torques (2.5, 3.5, and 4.5 kg·m) for disc (G95) at the end of slipping time at the outer radius from interface contact between the pressure plate and friction clutch disc ($t_s = 30$ s and $\omega_{ro} = 1200$ rpm). While on the other side

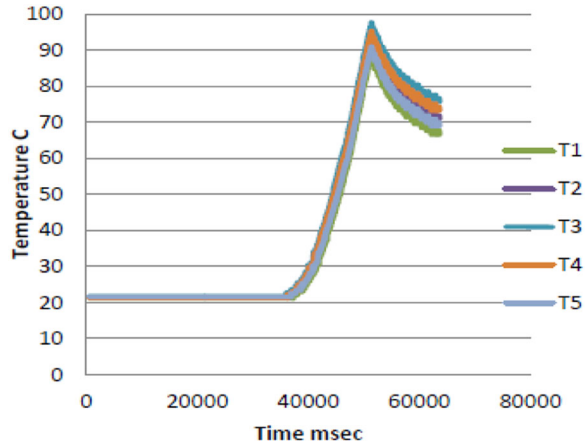

FIGURE 30 Temperature distribution on the pressure plate surface (slip time, 8 s; relative velocity, 680 rpm; and torque, 4.5 kg·m) for LUK disc

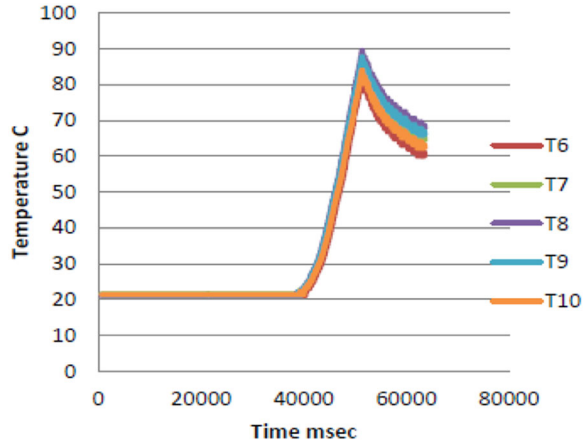

FIGURE 31 Temperature distribution on the flywheel surface (slip time, 8 s; relative velocity, 680 rpm; and torque, 4.5 kg·m) for LUK disc

(between the flywheel and friction disc) for the same operational conditions as shown in Figures 5, 13, and 21, it can be seen different values of temperatures which are 152.7°C, 127.3°C, and 114.8°C. The reason for these differences between the two sides (pressure plate side and flywheel side) is the low thermal capacity of the pressure plate compared with the flywheel. Therefore, mechanical designers should spotlight on the pressure plate side rather than the flywheel side.

Also, for the same disc, it can be seen from Figures 28, 36, and 44 show that the maximum values of temperature for the same disc clutch when applying torques (2.5, 3.5, and 4.5 kg·m) for $t_s = 8$ s and $\omega_{ro} = 680$ rpm are 63.2°C, 72.1°C, and 79.6°C at pressure plate side. While, on the flywheel side, the values of temperature are found (57.9°C, 64.4°C, and 70.1°C) as shown in Figures 29, 37, and 45, respectively.

Figures 6, 14, and 22 show the variation of temperature for the interface between the pressure plate and LUK clutch disc, and $t_s = 30$ s and $\omega_{ro} = 1200$ rpm. The maximum values of

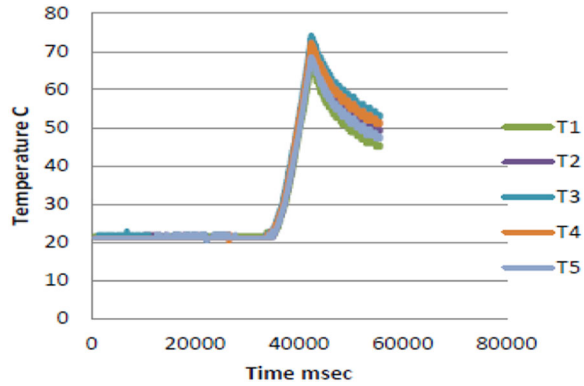

FIGURE 32 Temperature distribution on the pressure plate surface (slip time, 8 s; relative velocity, 680 rpm; and torque, 4.5 kg·m) for HCC disc

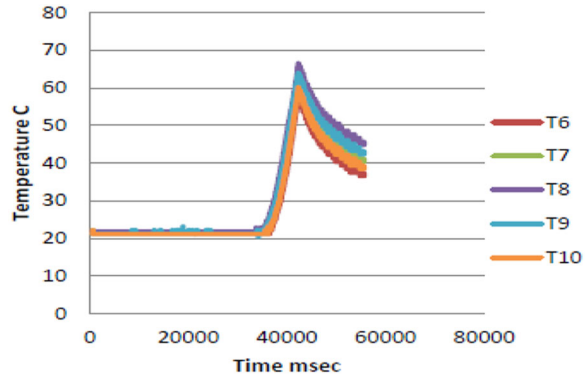

FIGURE 33 Temperature distribution on the flywheel surface (slip time, 8 s; relative velocity, 680 rpm; and torque, 4.5 kg·m) for HCC disc

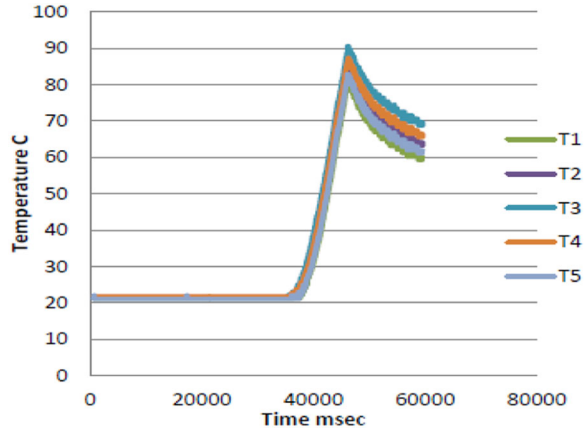

FIGURE 34 Temperature distribution on the pressure plate surface (slip time, 8 s; relative velocity, 680 rpm; and torque, 4.5 kg·m) for Tiger disc

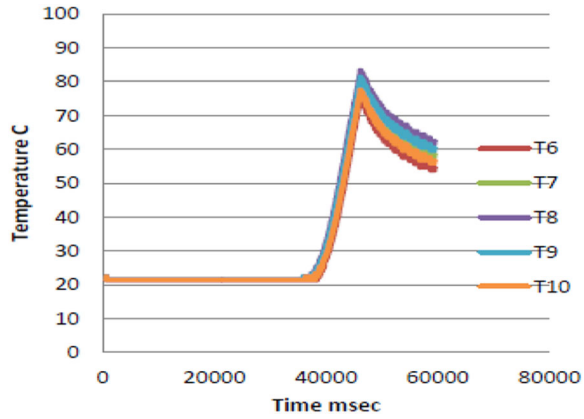

FIGURE 35 Temperature distribution on the flywheel surface (slip time, 8 s; relative velocity, 680 rpm; and torque, 4.5 kg·m) for Tiger disc

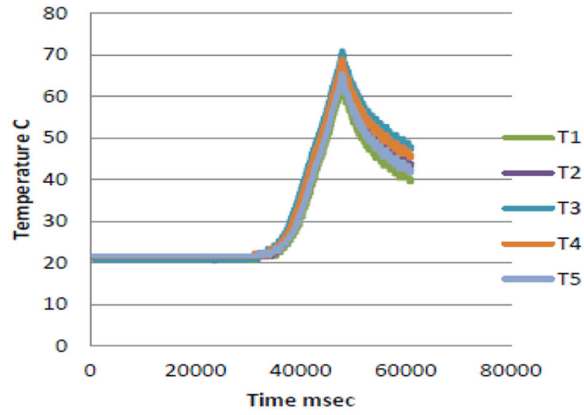

FIGURE 36 Temperature distribution on the pressure plate surface (slip time, 8 s; relative velocity, 680 rpm; and torque, 3.5 kg·m) for G95 disc

temperature are found (138°C, 152.9°C, and 180.4°C) corresponding to the applying torques (2.5, 3.5, and 4.5 kg·m), respectively. However, on the flywheel side, the maximum values of temperature are found (126.9°C, 145.8°C, and 171.2°C) that correspond to the applying torques (2.5, 3.5, and 4.5 kg·m), respectively as shown in Figures 7, 15, and 23. Figures 30, 38, and 46 that the maximum values of temperature when applying torques (4.5, 3.5, 2.5 kg·m) and ($t_s = 8$ s and $\omega_{ro} = 680$ rpm) are found to be (83.3°C, 90.9°C, and 98.6°C) on the pressure plate side. While, the maximum values of temperature on the flywheel side when applying the same values of torque are found (76.2°C, 82.9°C, and 89.6°C) as seen from Figures 31, 39, and 47, respectively.

Figures 8, 16, and 24 illustrate the variation of temperature for the interface between the pressure plate and HCC clutch disc under the same applying torques and $t_s = 30$ s and $\omega_{ro} = 1200$ rpm. It was found that the maximum temperatures that occurred on the pressure plate side are 118.9°C, 129.2°C, and 151.7°C, corresponding to the applying torques 2.5, 3.5, and 4.5 kg·m, respectively. However, the maximum values of temperature on the flywheel side

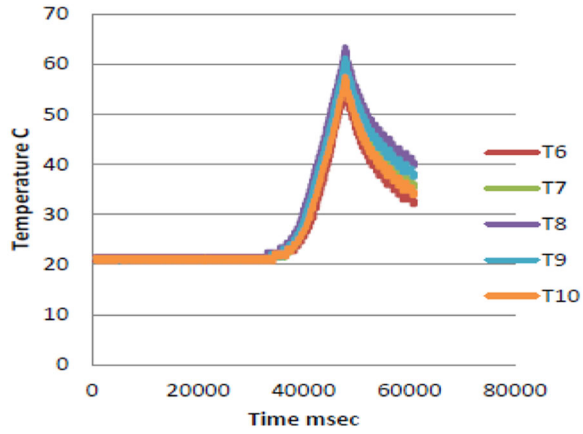

FIGURE 37 Temperature distribution on the flywheel surface (slip time, 8 s; relative velocity, 680 rpm; and torque, 3.5 kg·m) for G95 disc

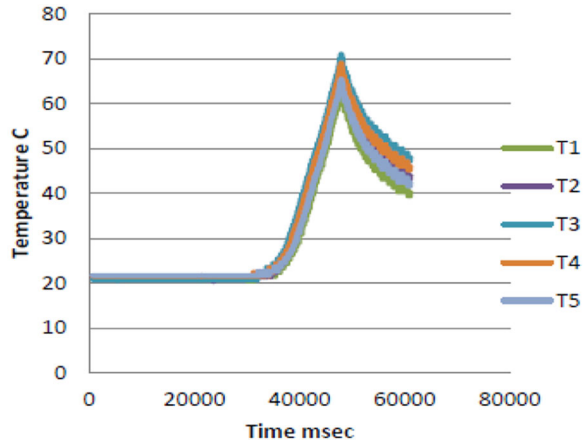

FIGURE 38 Temperature distribution on the pressure plate surface (slip time, 8 s; relative velocity, 680 rpm; and torque, 3.5 kg·m) for LUK disc

when applying the same values of torque are found (110.4°C, 120.3°C, and 143.9°C) as shown in Figures 9, 17, and 25. For the same applying torques and material (HCC) but other operational working conditions ($t_s = 8$ s and $\omega_{ro} = 680$ rpm), the maximum temperature for pressure plate side is found to be 55.7°C, 64.2°C, and 74.4°C corresponding to the applying torques (2.5, 3.5 and 4.5 kg·m), respectively, as shown in Figures 32, 40, and 48. While, the maximum values of temperature on the flywheel side when applying the same values of torque are found (49.3°C, 58.6°C, and 66.6°C) as shown in Figures 33, 41, and 49.

In case when using the other frictional material (Tiger) and ($t_s = 30$ s and $\omega_{ro} = 1200$ rpm), it was found that the maximum temperatures are 131.3°C, 143.7°C, and 170.2°C on the pressure plate side and 131.3°C, 143.7°C, and 170.2°C corresponding to the applying torques (2.5, 3.5, and 4.5 kg·m), respectively as shown in Figures 10, 18, and 26. On the other hand as presented in Figures 11, 19, and 27., the maximum temperatures on the flywheel side are found (122.4°C, 134.1°C, and 158.1°C). For the second operational conditions ($t_s = 8$ s and $\omega_{ro} = 680$ rpm), the

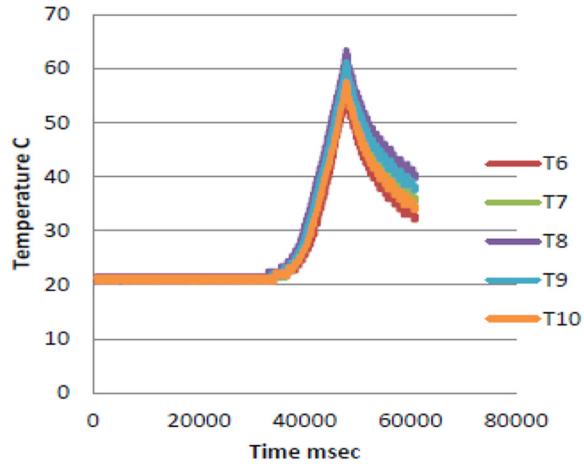

FIGURE 39 Temperature distribution on the flywheel surface (slip time, 8 s; relative velocity, 680 rpm; and torque, 3.5 kg·m) for LUK disc

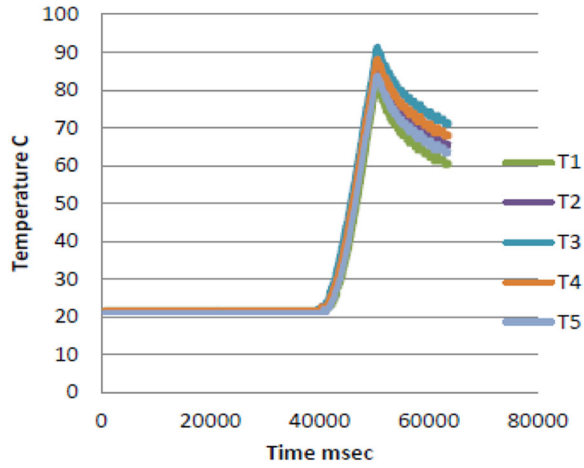

FIGURE 40 Temperature distribution on the pressure plate surface (slip time, 8 s; relative velocity, 680 rpm; and torque, 3.5 kg·m) for HCC disc

maximum temperatures for the pressure plate side are 75.1°C, 81.7°C, and 90.6°C as shown in Figures 34, 42, and 50, and on the flywheel are 67.9.4°C, 74.3°C, and 83.4°C as seen from Figures 35, 43 and 51 when applying torques for both cases are 2.5, 3.5, and 4.5 kg·m, respectively.

Based on the obtained results for all friction discs materials (G95, LUK, HCC, and Tiger), it can be observed "that the surface temperature grows linearly from minimum values at the inner disc radius to the maximum values at outer disc" radius. Generally, it can be noticed that the temperature values increase from the initial temperature at (T_i) to the maximum temperature T_{max} approximately before the end of the slipping period (heating phase). Later on, the temperatures decrease from T_{max} to final temperature during the full engagement period (cooling phase), until the temperature stabilizes at a certain value.

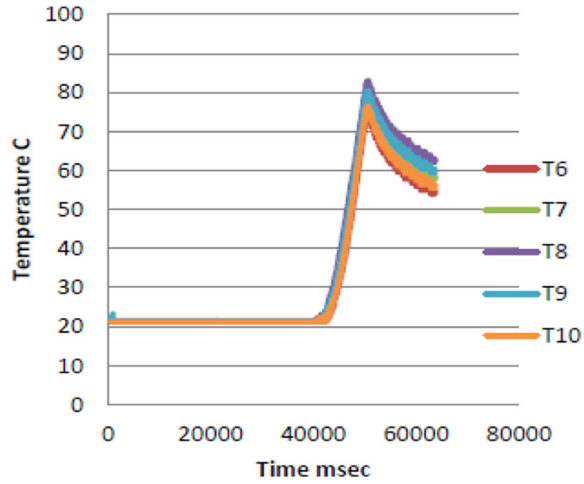

FIGURE 41 Temperature distribution on the flywheel surface (slip time, 8 s; relative velocity, 680 rpm; and torque, 3.5 kg·m) for HCC disc

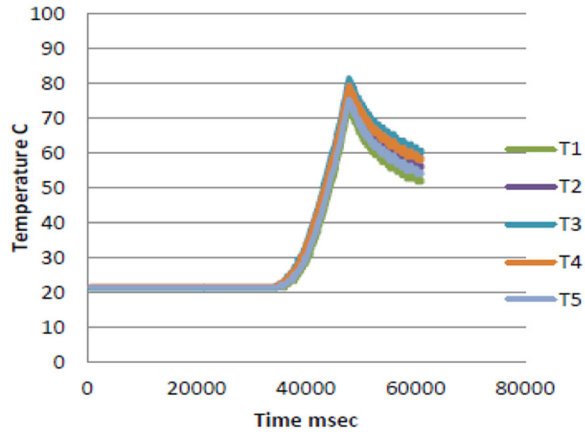

FIGURE 42 Temperature distribution on the pressure plate surface (slip time, 8 s; relative velocity, 680 rpm; and torque, 3.5 kg·m) for Tiger disc

For example (Figure 8) for HCC material ($T = 4.5$ kg·m, $t_s = 30$ s & $\omega_{ro} = 1200$ rpm), the initial temperature T_i was 21.2°C and then increased due sliding to maximum value approximately $T_{\max} = 143.9$°C, and at the end of sliding period the final temperature is $T_f = 124.3$°C. However, during the full engagement period (cooling phase) all clutch parts rotate together and the amount of heat generated on the rubbing surface gradually decreases and approaches to zero at the end of the slip period.

The small thermal capacity of the pressure plate causes to increase the surface temperature rapidly and will reach it to high values during a short time. Therefore, the results proved that for all cases, the surface temperature for the pressure plate was higher than those for the flywheel side. The other significant parameter is the angular sliding velocity, where the surface temperature increased dramatically when increased rotational velocity and slip time. The highest temperatures appeared for $t_s = 30$ s and $\omega_{ro} = 1200$ rpm, and the lowest values for

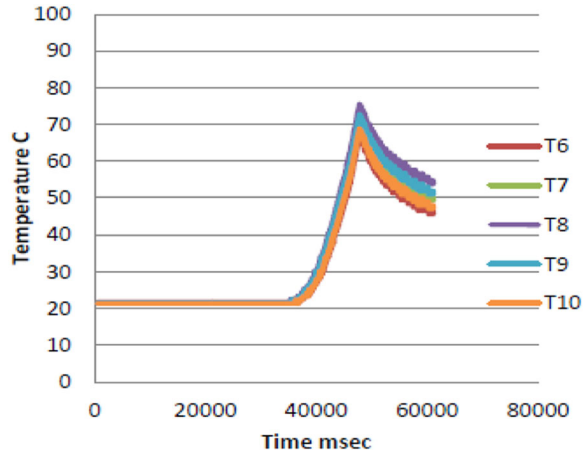

FIGURE 43 Temperature distribution on the flywheel surface (slip time, 8 s; relative velocity, 680 rpm; and torque, 3.5 kg·m) for Tiger disc

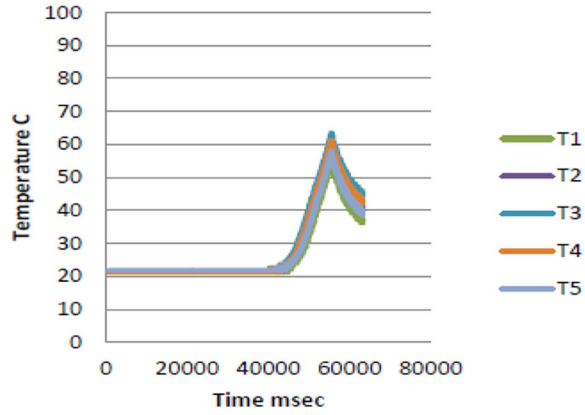

FIGURE 44 Temperature distribution on the pressure plate surface (slip time, 8 s; relative velocity, 680 rpm; and torque, 2.5 kg·m) for G95 disc

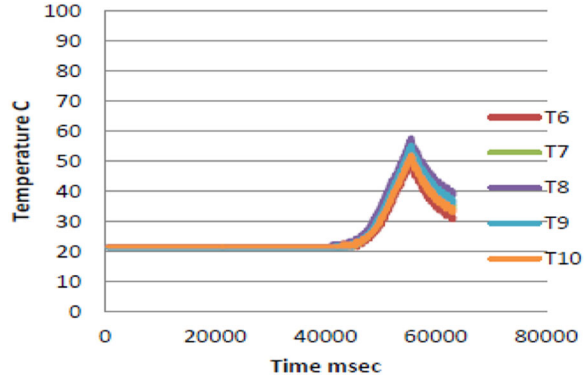

FIGURE 45 Temperature distribution on the flywheel surface (slip time, 8 s; relative velocity, 680 rpm; and torque, 2.5 kg·m) for G95 disc

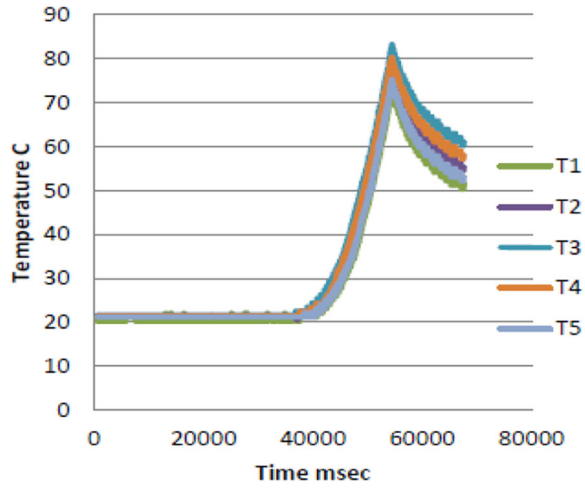

FIGURE 46 Temperature distribution on the pressure plate surface (slip time, 8 s; relative velocity, 680 rpm; and torque, 2.5 kg·m) for LUK disc

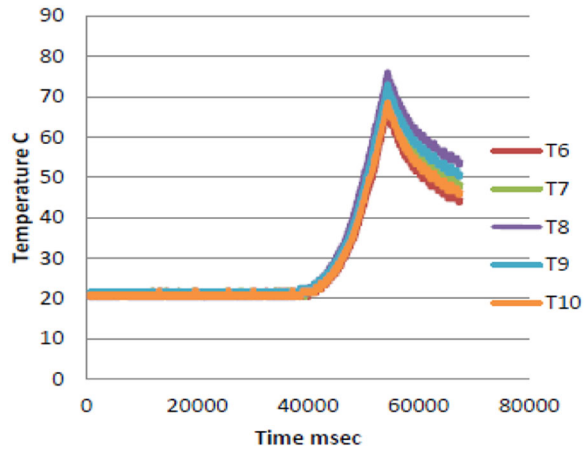

FIGURE 47 Temperature distribution on the flywheel surface (slip time, 8 s; relative velocity, 680 rpm; and torque, 2.5 kg·m) for LUK disc

$t_s = 8$ s and $\omega_{ro} = 680$ rpm when applying the same torque. Also, the torque plays an important role to specify the amount of heat generated, where the frictional heat generated is a function of applied torque. The maximum values of tempers for all cases occurred when applying the highest torque (4.5 kg·m), and the minimum one when applying the lowest torque (2.5 kg·m).

Figures 52 and 53 illustrate the temperature distribution with time at outer disc radius on the pressure plate and flywheel respectively, for case study ($t_s = 30$ s, $\omega_{ro} = 1200$ rpm, and 4.5 kg·m). While, Figures 54 and 55 show the temperature distribution with time at outer disc radius on the pressure plate and flywheel sides respectively for the case study ($t_s = 8$ s, $\omega_{ro} = 680$ rpm and 4.5 kg·m). It can be seen that the highest temperatures (180.4°C) appeared when using the LUK material and the lowest one (151.7°C) when using HCC frictional

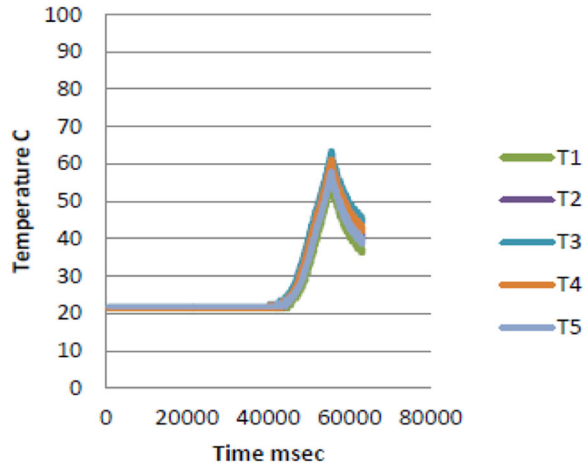

FIGURE 48 Temperature distribution on the pressure plate surface (slip time, 8 s; relative velocity, 680 rpm; and torque, 2.5 kg·m) for HCC disc

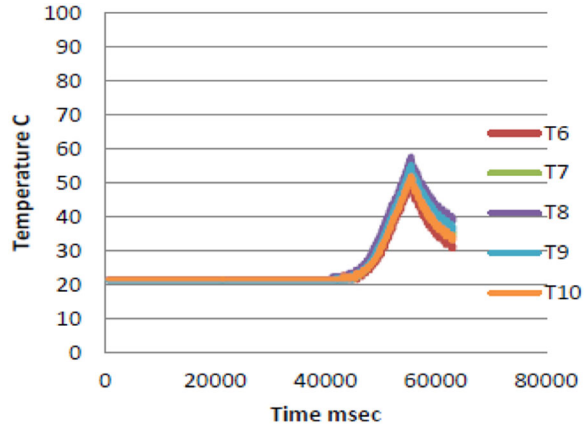

FIGURE 49 Temperature distribution on the flywheel surface (slip time, 8 s; relative velocity, 680 rpm; and torque, 2.5 kg·m) for HCC disc

material. The reason for such results is the poor thermal properties of LUK material compared with the HCC frictional material.

Also, it can be seen from Figures 56 and 57 for the case study ($t_s = 30$ s, $\omega_{ro} = 1200$ rpm and 4.5 kg·m), the variation of temperature with the disc radius when using G95 material on the pressure plate and flywheel sides, respectively. It is clear that the surface temperature grew linearly from minimum values at the inner disc radius to the maximum values at the outer disc radius. Where, the maximum temperature is 159.4°C occurred at outer radius ($r = 0.091$), and the minimum temperature is 150.9°C occurred at inner disc radius ($r = 0.064$ m) at the end of slipping time on the pressure plate side. However, on the flywheel side are found 139.6°C and 152.3°C) at inner and outer disc radii, respectively. These results are compatible with the theory of design for the friction clutch (uniform wear), where the maximum rate of water occurs at the outer radius and the minimum one at the inner radius. This trouble is considered one of the

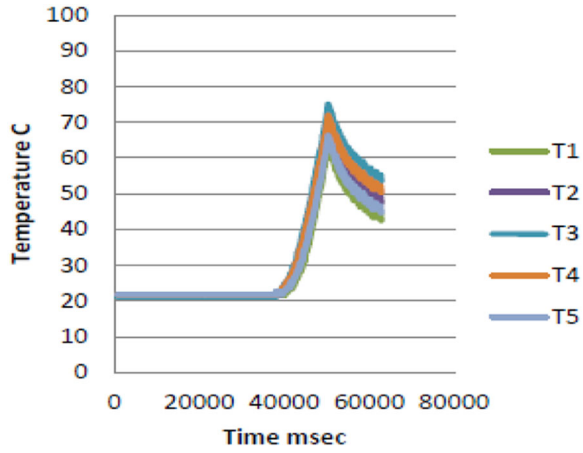

FIGURE 50 Temperature distribution on the pressure plate surface (slip time, 8 s; relative velocity, 680 rpm; and torque, 2.5 kg·m) for Tiger disc

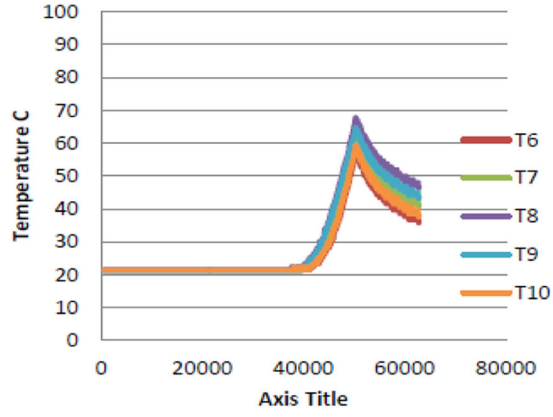

FIGURE 51 Temperature distribution on the flywheel surface (slip time, 8 s; relative velocity, 680 rpm; and torque, 2.5 kg·m) for Tiger disc

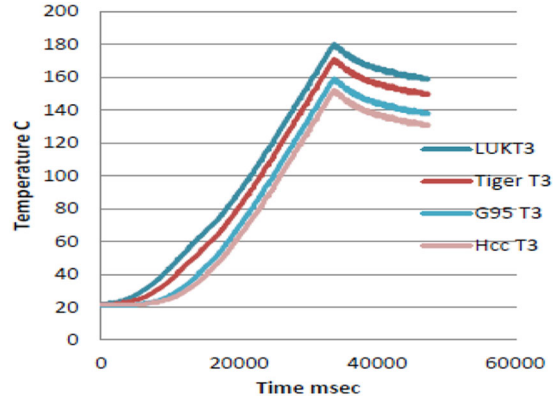

FIGURE 52 Temperature distribution on the pressure plate surface at outer disc radius (slip time, 30 s, relative velocity, 1200 rpm; and torque, 4.5 kg·m) for Discs (G95- LUK -HCC- Tiger)

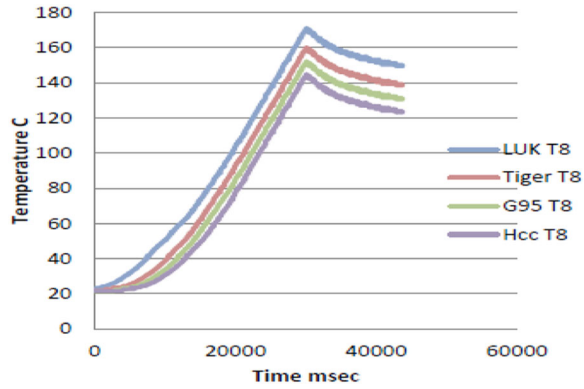

FIGURE 53 Temperature distribution on the flywheel surface at outer disc radius (slip time, 30 s; relative velocity, 1200 rpm; and torque, 4.5 kg·m) for discs (G95- LUK -HCC- Tiger)

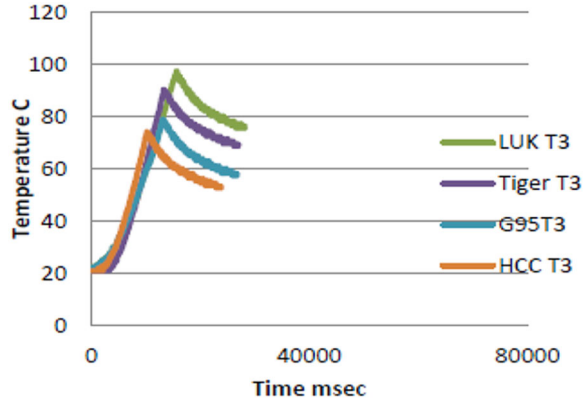

FIGURE 54 Temperature distribution on the pressure plate surface at outer disc radius (slip time, 8 s; relative velocity, 680 rpm; and torque, 4.5 kg·m) for discs (G95- LUK -HCC- Tiger)

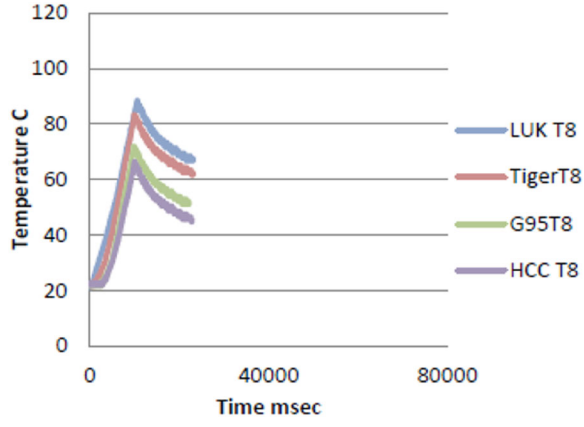

FIGURE 55 Temperature distribution on the flywheel surface at outer disc radius (slip time, 8 s; relative velocity, 680 rpm; and torque, 4.5 kg·m) for discs (G95- LUK -HCC- Tiger)

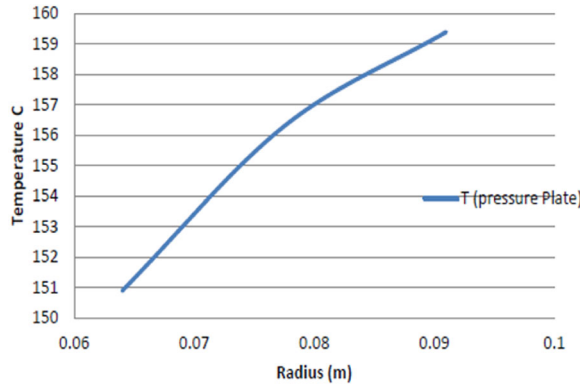

FIGURE 56 Temperature distribution on the pressure plate surface with radius (relative velocity, 1200 rpm; torque, 4.5 kg·m; and slip time, 30 s) for G95 disc

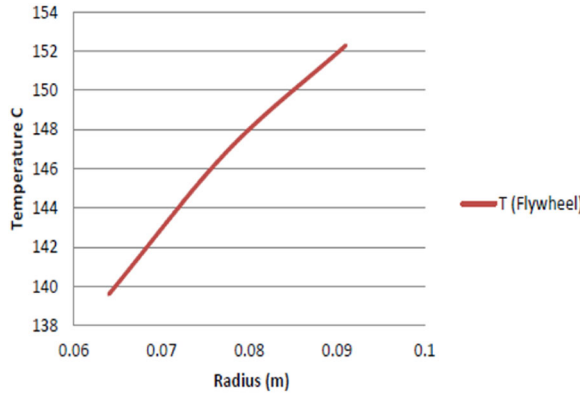

FIGURE 57 Temperature distribution on the flywheel surface with radius (relative velocity, 1200 rpm; torque, 4.5 kg·m; and slip time, 30 s) for G95 disc

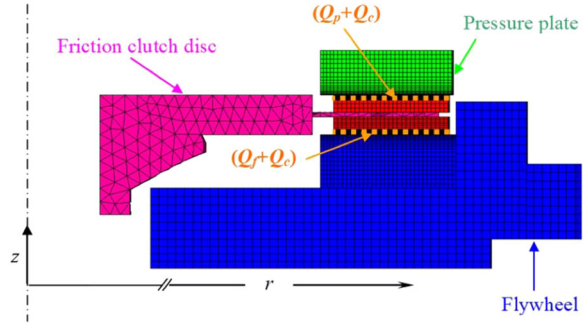

FIGURE 58 FE thermal model with the boundary conditions of dry friction clutch

TABLE 3 The maximum surface temperature (°C) on the pressure plate surface at r_o ($t_s = 30$ s, $\omega_{ro} = 1200$ rpm, and torque = 4.5 kg·m)

	Maximum surface temperature		
Type of material	**Numerical**	**Experimental**	**Diff. %**
G95	150.2	159.1	5.92
LUK	169.3	180.4	6.55
HCC	143.9	151.7	5.42
Tiger	159.7	170.2	6.57

main problems that lead to reducing the performance and lifetime of the frictional facing of the clutch disc.

To verify the results obtained for the experimental work, a finite element model (axisymmetric) was developed to achieve this task. Figure 58 shows the details of the finite element model and it was used the HCC material. Table 3 shows the comparison between the numerical and experimental results for the maximum surface temperature on the pressure plate surface at the outer disc radius. It can be seen that the maximum difference between these results is not exceeding 6.6%. Where, these differences are considered acceptable due to many factors that affected the accuracy of the experimental results such as accuracy of the degree of cooling, surface roughness, homogeneity assumption for materials, the accuracy of clutch elements, and so forth.

5 | CONCLUDING REMARKS

In this study paper, it was designed and built a new test rig to investigate the thermal behavior and performance of the dry friction clutches. Where, this test rig has the ability to provide full details of torque, temperature, and pressure, sliding speed during the slipping time. The most important conclusions that were found based on the present work are:

- The maximum temperature values occur when applying maximum torque (4.5 kg·m), it is observed that the temperature values increase with time when the values of applied torque increase.
- The surface temperature grows linearly from minimum values at the inner disc radius to the maximum values at the outer disc radius, where this finding is compatible with analytical and numerical results.
- The temperatures of the pressure plate interface are higher than those at the flywheel interface, because of the "low thermal capacity" of the pressure plate compared with the flywheel (volume of the flywheel is greater than the volume of the pressure plate).
- The highest temperature was obtained at maximum rotation speed and slip time (1200 rpm, 30 ms), and the lowest value was obtained when applying initial rotation speed and slip time (680 rpm, 8 ms).
- The HCC friction material has better thermal behavior in the sliding phase in relation to the three other materials (G95, LUK, and Tiger).
- The minimum temperatures were obtained when using friction clutch disc material (HCC), and maximum temperatures were obtained when using material (LUK).

ACKNOWLEDGMENT

The authors acknowledge the Mech. Engr. Dept./College of Engr.—the University of Baghdad for supporting the research work and providing facilities. Open access funding enabled and organized by Projekt DEAL.

REFERENCES

1. Barber JR. The influence of thermal expansion on the friction and wear process. *Wear*. 1967;10(2):155-159.
2. Barber JR. Thermoelastic instabilities in the sliding of conforming solids. *Proc R Soc Ser A Math Phys Sci*. 1969;312:381-394.
3. Santini JJ, Kennedy FE, Jr. An experimental investigation of surface temperatures and wear in disk brakes. Proceedings of the International Conference of Joint Lubrication, Montreal; 1974.
4. Anderson AE, Knapp RA. Hot spotting in automotive friction systems. *Wear*. 1990;135(2):319-337.
5. Panier S, Dufrénoy P, Weichert D. An experimental investigation of hot spots in railway disc brakes. *Wear*. 2004;256:764-773.
6. Abdullah O, Schlattmann J. Temperature analysis of a pin-on-disc tribology test using experimental and numerical approaches. *Friction*. 2016;4(2):135-143.
7. Mouffak E, Bouchetara M. Transient thermal behavior of automotive dry clutch discs by using Ansys Software. *MECHANIKA*. 2016;22(6):562-570.
8. Ali A, Ali L, Shah SR, Khan M, Imran SH, Butt SI. Dry friction clutch disc of an automobile under transient thermal load: a Comparison of friction lining materials. *MATEC Web Conf*. 2017;124:07003.
9. Gkinis T, Rahmani R, Rahnejat H, O′Mahony M. Heat generation and transfer in automotive dry clutch engagement. *J Zhejiang Univ Sci A*. 2018;19:175-188.
10. Abdullah OI, Majeed MH, Hussain IY. Effects of frictional facing thickness on the heat generated in dry friction clutches. *IOP Conf Ser Mater Sci Eng*. 2018;433:012044.
11. Sherza JS, Hussain IY, Abdullah O. Heat flux in friction clutch with time dependent torque and angular velocity. International Conference on Advanced Science and Engineering (ICOASE). IEEE, Kurdistan Region; 2018.
12. Sherza JS, Hussain IY, Abdullah O. Finite element simulation of thermal behavior of dry friction clutch system during the slipping period. *J Mech Contin Math Sci*. 2019;14(4):41-58.
13. Al-Zubaidi S, Abdullah O. Investigation of thermal influence on the frictional characteristics of friction materials. *J Balk Tribol Assoc*. 2020;26(3):14-29.
14. Biczó R, Kalácska G, Mankovits T. Micromechanical model and thermal properties of dry-friction hybrid polymer composite clutch facings. *Materials*. 2020;13(20):1-25.
15. AL-Alawi A, Yousif AE, Jassim MAH. An investigation into the behavior of disc brake wear. *Al-Khwarizmi Eng J*. 2007;3(2):49-66.
16. Rohan Ramesh M, Atharva Ravindra K, Ashok B, Kannan C. Optimizing thermal performance of a dry rigid clutch by varying groove pattern and friction material. *Mater Today Proc*. 2021;46:7459-7467.
17. Bhaduri S, MuruguNachippan N. A numerical analysis of friction plate on automotive clutch system. *Int J Adv Eng Res Dev*. 2017;4(1):275-281.
18. Bhandari N, Mane PR. Finite element analysis of thermal buckling in automotive clutch plate disc. *Int J Sci Res Dev*. 2020;8(2):306-310.
19. Harish K, Kumar YD. Optimization of friction clutch for various friction. *Materials*. 2017;4(17):3493-3498.

How to cite this article: Sherzaa JS, Hussain IY, Abdullah OI. Experimental investigation of transient thermal characteristics of a dry friction clutch using alternative friction materials under different operating conditions. *Heat Transfer*. 2022;51:3920-3950. doi:10.1002/htj.22483